Quasielastic scattering of pions from ^{12}C and $^{40,44,48}Ca$

G. R. Burleson and G. S. Blanpied*
New Mexico State University, Las Cruces, New Mexico 88003

J. Davis, J. S. McCarthy, and R. C. Minehart
University of Virginia, Charlottesville, Virginia 22901

C. Goulding
Florida A&M University, Tallahassee, Florida 32306

C. L. Morris and H. A. Thiessen
Los Alamos Scientific Laboratory, Los Alamos, New Mexico 87545

W. B. Cottingame, S. Greene, and C. F. Moore
University of Texas, Austin, Texas 78712
(Received 11 September 1979)

Measurements have been made of the differential cross section $d^2\sigma/d\Omega dE$ for the scattering of $\pi^{\pm}$ from ^{12}C and $^{40,44,48}Ca$ in the energy region corresponding to quasielastic scattering. Data were taken at incident energies and laboratory angles of 180 MeV, 60°, and 290 MeV, 60° and 120°. The results are compared to a free pion-nucleon cross-section model and to a model based on pion scattering from a Fermi gas of nucleons, which incorporates free pion-nucleon cross sections. Monte Carlo methods were used for the second model, and both single scattering and multiple scattering were allowed. Several qualitative features of the data are explained by the multiple scattering calculation, but not by the free cross-section model or the single scattering model.

[NUCLEAR REACTIONS Quasielastic scattering of $\pi^{\pm}$ from ^{12}C and $^{40,44,48}Ca$ at 291 MeV, 60° and 120°, and 180 MeV, 60°. Model of data based on Monte Carlo calculation of scattering from Fermi gas of nucleons, with multiple scattering, using free pion-nucleon cross sections calculated from phase shifts.]

I. INTRODUCTION

One of the principal contributions to the scattering of medium-energy particles from nuclei is the $(\pi, \pi N)$ quasielastic (or quasifree) process. By this, we mean a (perhaps idealized) process in which the incident particle knocks a nucleon out of a nucleus in such a way that there is no major interaction between the nucleus and the incident or the two outgoing particles. Quasielastic scattering has been the subject of much experimental and theoretical investigation, principally with protons and electrons. With these projectiles, two types of experiments have been carried out, single-arm measurements, in which only the scattered particle is detected, and double-arm ones, in which the knocked-out nucleon is detected as well. There have been several good reviews of this subject, of which one of the latest is Ref. 1.

The scattering of electrons is perhaps the best example of this process, since electrons are weakly interacting particles and have a long mean free path in nuclear matter. The results of the single-arm measurements have generally been very well represented by a fairly simple model of scattering from a degenerate Fermi gas of nucleons[2]; scattering data of Li through Pb have been successfully fitted[3] with a model involving two parameters, the nuclear Fermi momentum and the average nucleon interaction energy.

For protons, however, the mean free path in nuclear matter is small enough that it is fairly likely that more than a single scattering will take place before the incident particle can leave the nucleus, so that the interaction might be described crudely as a sequence of independent nucleon-nucleon collisions. These multiple-scattering events form an important background to the quasielastic (single collision) process. Any theoretical description of such a process must take into account these effects, as well as the distortion effects corresponding to the strong nucleon-nucleon interaction.[1]

The process of pion quasielastic scattering has recently been the subject of much theoretical and experimental investigation. For pion energies near the (3,3) resonance, multiple scattering and distortion effects are expected to be even stronger than for protons, since the mean free path of pions in this energy region is smaller. A discussion of quasielastic pion scattering in this energy region

was recently given by Silbar.[4] Some of the earliest studies of this involved measurements of the total cross sections for the $^{12}C(\pi^{\pm},\pi^{\pm}n)^{11}C$ reactions, using radiochemical methods.[5] A simple impulse approximation model, which neglects multiple scattering, together with isospin considerations, predicts the ratio of the π^- to π^+ cross sections to be 3.0 near the peak of the resonance, whereas experimentally it was found to be no greater than about 1.8. Later studies[6] found similar discrepancies in other nuclei, from ^{4}He to ^{64}Zn. Several mechanisms have been proposed to explain these results; a summary of them is given in Ref. 7. One of the more successful of these mechanisms has involved detailed considerations of the effect of charge exchange of the outgoing nucleon.[8] Other effects which may contribute that have been studied include coherent mixing between nuclear states of different isospin,[9] the formation of "quasialpha particles",[10] enhancements in particular two-particle isospin states in the three-particle final state,[11] and the distortion of the incoming and outgoing pion, with the use of different off-shell extrapolations.[12]

Recently, several experiments have been carried out involving studies of pion quasielastic scattering near the (3,3) resonance by using counter techniques. Swenson *et al.*,[7,13] used both single-arm (for nucleon detection) and double-arm methods, with ^{27}Al and ^{208}Pb targets, and with both signs of pion charge, but with no energy measurements of the scattered pion. They interpret their results as supporting the view that charge exchange of the outgoing nucleon plays an important role in this process, but that further studies are needed to confirm this. Some results of measurements on ^{16}O involving detection of the scattered pion in a spectrometer have been reported by Ingram *et al.*[14] The effects of multiple scattering were clearly seen in these data, and estimates of its magnitude and characteristics were made by using comparisons with (e,e') and (π^+,π^-) data on ^{16}O in the quasielastic region.

In this paper, we report the results of a one-arm measurement of the differential cross section $d^2\sigma/d\Omega dE$ for $\pi^{\pm}$ scattered from ^{12}C and ^{40,44,48}Ca in the quasielastic energy region, using a magnetic spectrometer to detect the pion. Data were taken at 180 MeV, 60°, and 290 MeV, 60° and 120°.

II. EXPERIMENTAL METHOD

These measurements were made using the EPICS[15] facility at LAMPF. Eleven overlapping momentum bites were used to detect the scattered pions at energies from 291 to 50 MeV. Elastic data on hydrogen were taken at each spectrometer setting in order to measure the absolute cross section as well as the background. These calibration measurements were made with CH_2 (140 mg/cm^2) and graphite (230 mg/cm^2) targets so that the ^{12}C background could be directly subtracted to yield the hydrogen peak and its associated background, which was presumably due principally to muons from pion decays in the spectrometer dipoles. Measurements confirmed that the background from a given hydrogen peak remained correlated in energy and did not "spill over" into the other spectrometer settings. The background was found to be a constant fraction of the detected pions, independent of their energy. The resulting reduction factor for the data was 0.94 ± 0.01 (0.88 ± 0.06) for a π^+ (π^-) beam. The cross sections for pion-proton scattering predicted by the phase shifts of Rowe *et al.*,[16] were used to normalize the data.

Strip targets of ^{12}C and ^{40,44,48}Ca, of vertical height about 4 cm and of thicknesses 476, 249, 146, and 202 mg/cm^2, were used. These were arranged vertically to make one single target array that intercepted the pion beam spot, which was approximately 20×10 cm. The paths of the pions detected by the spectrometer system were projected back to the target with a resolution of about ±0.3 cm, which was sufficient to determine cleanly which target they were scattered from. Fairly conservative software cuts were used that limited the accepted events to the center 2.5 cm of each strip; another cut limited the scattered angular acceptance to 3°. Since the beam profile on the target was not uniform, these same cuts were used for the CH_2 and graphite targets as well. A separate normalization for each strip was thus obtained. These cuts, plus the requirement of 12 good checks of the wire chambers in the detection system, resulted in a reduction of the number of events accepted to about 20% of the online events. The calculated energies of the scattered pions were initially put into bins of width 0.2 MeV/channel and later recombined into bins of width 3.0 MeV/channel, for which the cross sections described below were calculated.

The absolute errors due to uncertainties in the normalization, background subtraction, and target thickness for π^+ (π^-) on ^{12}C, ^{40}Ca, ^{44}Ca, and ^{48}Ca are 9.2 (11.0), 4.2 (7.3), 4.7 (7.6), and 4.1 (7.2)%, respectively. The "flat" portion of the spectrometer acceptance as a function of pion energy loss was used for all data. The variation of acceptance with energy loss in this region was found to be a small effect, compared with the statistical errors.

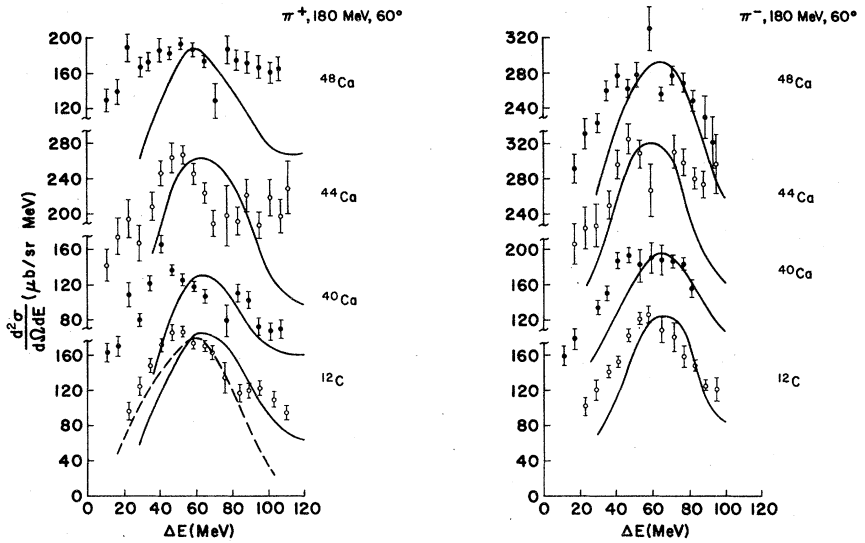

FIG. 1. Experimental values of the cross section $d^2\sigma/d\Omega dE$ of $\pi^{\pm}$ scattered quasielastically from ^{12}C, ^{40}Ca, ^{44}Ca, and ^{48}Ca at 180 MeV, 60°. The solid curves are predictions of a Monte Carlo calculation, with multiple scattering, of pion scattering from a Fermi gas of nucleons uniformly distributed within a sphere of radius $1.2\,A^{1/3}$ fm. The dashed curve is the prediction of the same calculation for π^- on ^{12}C, with no multiple scattering. The theoretical curves are normalized to have roughly the same peak height as the experimental curves.

III. RESULTS

The resulting cross sections $d^2\sigma/d\Omega dE$ are shown in Figs. 1–3. The curves in these figures are predictions of a Fermi gas model discussed below. The errors shown are statistical.

Values of various ratios of these cross sections are presented in Tables I and II. For each case, the ratio given is an average of the point-by-point ratios over the entire experimental curve, weighted by the statistical errors. The value of χ^2 per degree of freedom for this average ratio, compared to the individual ones, was near unity in most cases. Table I presents the value of the π^-/π^+ ratio for each pair of curves at a given energy and angle. With a self-conjugate nucleus, this ratio should be 1, if Coulomb effects are negligible. For ^{12}C and ^{40}Ca, this ratio is consistent with

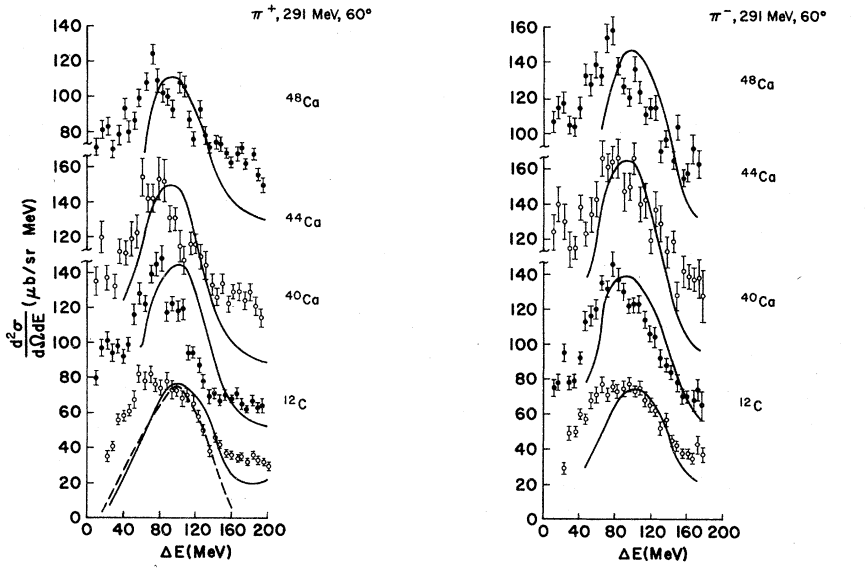

FIG. 2. Same as Fig. 1, except for 291 MeV, 60°.

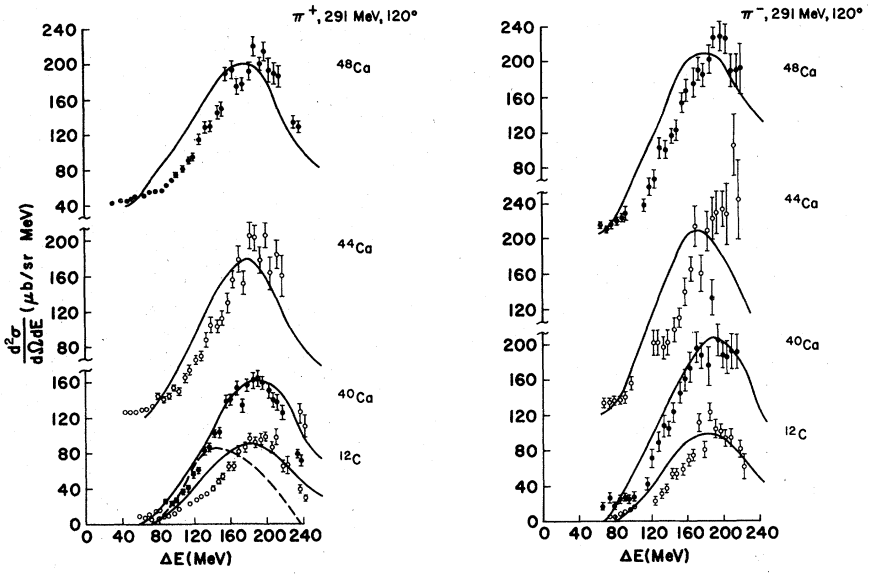

FIG. 3. Same as Fig. 2, except for 291 MeV, 120°.

unity, except for ^{40}Ca at 291 MeV, 120°, where it is 1.22. Table II presents the ratios of the cross sections for ^{44}Ca and ^{48}Ca to that for ^{40}Ca. Also given in these tables are predictions for these ratios from a simple model based on free pion-nucleon cross sections, and from two forms of a Fermi gas model, both of which are described below.

The free cross-section model

To first (or zeroth) order, it is expected that quasielastic scattering could be described by pion scattering from a collection of Z protons and N neutrons having a Fermi distribution of momenta, and that the pion-nucleon cross sections averaged over this distribution should give results near the free values. Such a model would give the following simple prediction for the energy-integrated quasielastic cross section:

$$\frac{d\sigma}{d\Omega} = N_{\text{eff}} \frac{Z(d\sigma/d\Omega)_p + N(d\sigma/d\Omega)_n}{A},$$

where $(d\sigma/d\Omega)_{p,n}$ are the free$(\pi - p)$ and $(\pi - n)$ cross sections, $A = N + Z$, and N_{eff} is the effective number of nucleons (to be determined from the data). Predictions of this simple model for various ratios (assuming N_{eff} constant at a given energy) are given in Tables I and II as R_{free}. The free cross

TABLE I. Experimental and theoretical value of the π^-/π^+ ratios $R^{(\text{charge})}$ of the quasielastic cross sections. The experimental values are a weighted average of the point-by-point ratios. The sources of the theoretical values are described in the text; the errors indicated arise from the Monte Carlo process.

T_π (MeV)	θ	Nucleus	$R_{\text{exp}}^{(\text{charge})}$	$R_{\text{mult}}^{(\text{charge})}$	$R_{\text{single}}^{(\text{charge})}$	$R_{\text{free}}^{(\text{charge})}$
180	60°	^{12}C	1.03 ± 0.02	(1.0)	0.98 ± 0.04	1.0
		^{40}Ca	1.03 ± 0.02	(1.0)	0.99 ± 0.04	1.0
		^{44}Ca	1.25 ± 0.04	1.12 ± 0.07	1.08 ± 0.04	1.16
		^{48}Ca	1.42 ± 0.04	1.30 ± 0.08	1.12 ± 0.04	1.31
291	60°	^{12}C	1.00 ± 0.02	(1.0)	0.98 ± 0.04	1.0
		^{40}Ca	1.03 ± 0.02	(1.0)	0.98 ± 0.04	1.0
		^{44}Ca	1.15 ± 0.02	1.12 ± 0.05	1.03 ± 0.04	1.13
		^{48}Ca	1.31 ± 0.02	1.35 ± 0.07	1.16 ± 0.04	1.25
291	120°	^{12}C	1.03 ± 0.03	(1.0)	1.00 ± 0.05	1.0
		^{40}Ca	1.22 ± 0.03	(1.0)	1.07 ± 0.05	1.0
		^{44}Ca	1.07 ± 0.04	1.16 ± 0.04	1.09 ± 0.05	1.13
		^{48}Ca	1.24 ± 0.03	1.48 ± 0.06	1.17 ± 0.05	1.24

TABLE II. Experimental and theoretical values of ratios $R^{(\text{isotope})}$ of the quasielastic cross sections of the isotopes ^{44}Ca and ^{48}Ca to ^{40}Ca. The experimental values are a weighted average of the point-by-point values. The sources of the theoretical values are described in the text; the errors indicated arise from the Monte Carlo process.

Pion	T_π (MeV)	θ	Nucleus	$R_{\text{exp}}^{(\text{isotope})}$	$R_{\text{mult}}^{(\text{isotope})}$	$R_{\text{single}}^{(\text{isotope})}$	$R_{\text{free}}^{(\text{isotope})}$
π^-	180	60°	^{44}Ca	1.35 ± 0.03	1.05 ± 0.06	1.04 ± 0.04	1.07
			^{48}Ca	1.22 ± 0.02	1.14 ± 0.05	1.03 ± 0.04	1.13
	290	60°	^{44}Ca	1.27 ± 0.12	0.97 ± 0.05	1.06 ± 0.04	1.06
			^{48}Ca	1.11 ± 0.03	1.07 ± 0.05	1.09 ± 0.04	1.11
	290	120°	^{44}Ca	0.94 ± 0.03	1.02 ± 0.04	1.01 ± 0.05	1.06
			^{48}Ca	1.02 ± 0.03	1.17 ± 0.05	1.06 ± 0.05	1.11
π^+	180	60°	^{44}Ca	1.19 ± 0.03	0.93 ± 0.05	0.95 ± 0.04	0.93
			^{48}Ca	0.93 ± 0.03	0.82 ± 0.05	0.92 ± 0.04	0.87
	290	60°	^{44}Ca	1.15 ± 0.12	0.88 ± 0.04	0.96 ± 0.04	0.94
			^{48}Ca	0.89 ± 0.02	0.79 ± 0.04	0.92 ± 0.04	0.89
	290	120°	^{44}Ca	1.09 ± 0.02	0.93 ± 0.05	1.00 ± 0.05	0.94
			^{48}Ca	1.02 ± 0.02	0.82 ± 0.04	0.97 ± 0.05	0.89

sections were calculated from the pion-nucleon phase shift fits of Rowe *et al.*[16]

The Fermi gas model

A more detailed calculation based on pion scattering from a Fermi gas of nucleons, similar to the one used for electron quasielastic scattering,[2,3] has also been made, using Monte Carlo methods. The nucleus was assumed to contain Z protons and N neutrons uniformly distributed inside a sphere of radius $R_0A^{1/3}$, having a Fermi momentum distribution, with the maximum (Fermi) momentum value taken from the fits to electron scattering results.[3] The direction of motion of the nucleons was taken to be isotropic. The interaction probabilities and angular distributions generated were based on free total and differential pion-nucleon cross sections calculated from phase shifts.[16] To account for nuclear binding, the struck nucleon was given a mass equal to the free nucleon mass reduced by the nuclear separation energy, but it was given a free mass after recoil; neutrons and protons were treated separately. Pion charge-exchange scattering was also included, which gave an energy-dependent depletion of the number of scattered pions. Coulomb effects were neglected.

The program was run both for single and multple scattering. For multiple scattering, the path of the pion was followed in detail through the nucleus for each event, and it was allowed to continue scattering, with interaction probabilities and angular distributions based on free pion-nucleon interactions, until it (1) emerged, (2) charge-exchanged, or (3) underwent a scattering which could not remove a nucleon from the nucleus, due to too low a pion energy. (For those cases in which either of the last two events occurred, the pion was considered lost.) For each type of scattering, the program recorded the energy distribution of the pions emerging within specified angular regions and calculated the resulting cross sections (per nucleon). About 50 000 events were run for the single scattering cases, and about 25 000 events for multiple scattering. The results of this calculation given in the tables therefore have statistical errors, which are indicated.

The calculation does not include many effects, of which the following might be mentioned:

(1) Pion absorption on nucleon pairs. A useful detailed description of this process is not currently available, and it is not clear how to best include it in the calculation. The principal effect (at a single energy) would be to reduce all cross sections by about the same factor, as well as to reduce multiple scattering. The single-scattering portion of the spectrum should not be affected by this, however.

(2) Variation of nuclear density. A more realistic density distribution, such as a Woods-Saxon model, would be preferable, but more difficult, to use. This would affect, of course, only the multiple-scattering calculations.

(3) The effect of the pion-nuclear optical potential. Presumably, off-shell values of pion-nucleon scattering should be used, though it is not clear that the on-shell values would not be preferable, for the case in which the nucleons are farther apart than the range of the pion-nucleon interaction.[4]

(4) The effect of nuclear correlations. Because the pion mean free path is the same order of magnitude as the internucleon distance, objections to the assumption of incoherence in the multiple-scattering process could be raised.

Some features of the multiple-scattering process as seen in the Monte Carlo program are presented in Table III. These include such quantities as the

TABLE III. Some features of the pion multiple-scattering process as seen in the Monte Carlo program.

Pion	T_π (MeV)	Nucleus	Pion mean free path (fm)	End results of pion cascade: Fraction escaping	Fraction charge exchanging	Fraction stopping	Fraction of pions that multiple scatter: 60°	120°
π^-	180	^{12}C	0.62	0.60	0.33	0.07	0.43	0.54
		^{40}Ca	0.68	0.54	0.40	0.07	0.42	0.62
		^{44}Ca	0.66	0.56	0.39	0.06	0.46	0.62
		^{48}Ca	0.65	0.57	0.37	0.06	0.44	0.61
	291	^{12}C	0.93	0.66	0.28	0.06	0.43	0.54
		^{40}Ca	1.08	0.57	0.36	0.07	0.46	0.58
		^{44}Ca	1.06	0.58	0.36	0.06	0.48	0.62
		^{48}Ca	1.03	0.58	0.35	0.07	0.48	0.63
π^+	180	^{44}Ca	0.70	0.53	0.43	0.04	0.44	0.57
		^{48}Ca	0.73	0.51	0.44	0.05	0.42	0.57
	291	^{44}Ca	1.15	0.56	0.40	0.04	0.43	0.56
		^{48}Ca	1.20	0.54	0.42	0.05	0.42	0.55

mean free path, the fraction of events which undergo more than a single scattering (at both 60° and 120°), and the fractions of events escaping from the nucleus, charge exchanging, and stopping due to low pion energy. It should be noted that in general the calculated fraction of events which undergo more than single scattering is large (about 50%), and that the pions emerging at 120° have generally undergone more multiple scattering than those emerging at 60°. We note that the fraction of multiple scattering seen in the calculation is greater than that estimated in Ref. 14. The fraction of pions undergoing many successive multiple scatterings is also found to be fairly large, with some events having as high as tenfold scattering before emerging.

The predictions of the calculation with multiple scattering are shown in Figs. 1–3 as the solid curves (which were smoothed by eye over the Monte Carlo output, which was in the form of a histogram). The value of R_0 used was 1.2 fm; results for $R_0 = 1.4$ fm are very similar. The dashed curves in these figures show the prediction for ^{12}C, allowing only single scattering; predictions for other nuclei are similar. The predicted curves are normalized so that the peaks lie roughly on the peaks of the experimental curves. Values of cross-section ratios predicted by this calculation (with N_{eff} constant for a given energy) are given in the Tables as R_{single} and R_{mult} for the single- and multiple-scattering cases, respectively.

Because the data were taken over less than the full range of scattered pion energy, it is difficult to integrate over the experimental curves to find $d\sigma/d\Omega$. In order to study these results further, however, a comparison of the experimental cross sections at the peaks was made with the predictions of the Monte Carlo calculations at the peaks. Because of the lack of detailed agreement between the experimental shapes and the Monte Carlo predictions of these shapes, however, the validity of this procedure is questionable, but it should give an idea of certain features of the quasielastic scattering process as described in this model. Table IV presents experimental and theoretical

TABLE IV. Experimental and theoretical values of the ratio $R^{(\text{angle})}$ of the cross sections at the peak of the quasielastic curve at 120° to that at 60° at 291 MeV. The errors indicated in the theoretical results arise from the Monte Carlo process.

Pion	Nucleus	$R_{\text{exp}}^{(\text{angle})}$	$R_{\text{mult}}^{(\text{angle})}$	$R_{\text{single}}^{(\text{angle})}$	$R_{\text{free}}^{(\text{angle})}$
π^-	^{12}C	1.19 ± 0.07	1.04 ± 0.07	0.50 ± 0.04	0.52
	^{40}Ca	1.18 ± 0.07	1.39 ± 0.09	0.44 ± 0.04	0.52
	^{44}Ca	1.33 ± 0.09	1.49 ± 0.10	0.46 ± 0.04	0.52
	^{48}Ca	1.48 ± 0.10	1.39 ± 0.10	0.47 ± 0.04	0.52
π^+	^{12}C	1.35 ± 0.09	1.04 ± 0.07	0.47 ± 0.04	0.52
	^{40}Ca	1.48 ± 0.10	1.39 ± 0.10	0.44 ± 0.04	0.52
	^{44}Ca	1.35 ± 0.09	1.48 ± 0.10	0.42 ± 0.04	0.52
	^{48}Ca	1.53 ± 0.11	1.56 ± 0.11	0.46 ± 0.04	0.52

values of the ratio of the quasielastic peak cross section at 120° to that at 60° for 291 MeV. (The free cross-section predictions here are based on ratios of $d\sigma/d\Omega$.) Table V presents the effective number of nucleons N_{eff} found by this procedure, where N_{eff} is taken to be the ratio between the experimental peak cross section and the peak cross section per nucleon predicted by the multiple-scattering calculation. We should note that these values should not be compared with the predictions of Ref. 4 for N_{eff}, since those were calculated for the pure quasielastic process.

Comparison of the data with the models

As is seen in Figs. 1–3, the multiple-scattering calculation does not predict the detailed shapes of the experimental curves, but it does account for the shift of the peak to lower energy than that predicted by single scattering at 291 MeV, 120°, as well as for the low-energy tails of the experimental curves. We believe that small-energy-loss portion of the 60° curves, which is not accounted for by the calculation, includes contributions from inelastic scattering leading to nuclear excitation.

The predictions of the Monte Carlo calculation and the free cross-section model for the ratios of Tables I and II are similar. For the π^-/π^+ ratios, the experimental results generally follow the predicted trend; the large value of this ratio for ^{40}Ca at 291 MeV, 120°, is not understood, however. For the ratios of ^{44}Ca and ^{48}Ca to ^{40}Ca in Table II, several unexpected features are seen. For the π^- results, the ^{44}Ca cross sections at 60° are greater than the ^{48}Ca cross sections, and the ^{44}Ca and ^{48}Ca cross sections at 120° (291 MeV) are nearly equal, in contrast to the predictions, which indicate that the cross sections should increase with neutron number. For the π^+ results, the ^{48}Ca cross sections are smaller than the ^{44}Ca cross sections, as predicted, but the ^{44}Ca cross sections are larger than the ^{40}Ca ones, which is not predicted.

TABLE V. Effective number of nucleons N_{eff} that participate in the quasielastic scattering process as determined by the ratio of the experimental cross section at the peak to the cross section per nucleon at the peak calculated by the multiple-scattering program. The error in N_{eff} as determined by this method is estimated to be about ±10%.

T_π (MeV)	θ	Nucleus	$N_{\text{eff}}(\pi^-)$	$N_{\text{eff}}(\pi^+)$
180	60°	^{12}C	3.8	3.6
		^{40}Ca	5.9	6.4
		^{44}Ca	8.1	7.5
		^{48}Ca	6.6	6.0
291	60°	^{12}C	5.6	5.8
		^{40}Ca	15.7	16.2
		^{44}Ca	18.6	17.2
		^{48}Ca	16.2	13.9
291	120°	^{12}C	7.3	6.6
		^{40}Ca	16.7	13.8
		^{44}Ca	17.0	15.4
		^{48}Ca	15.9	14.7

The results presented in Table IV show that the Monte Carlo multiple-scattering calculation fairly successfully reproduces another feature of the data, the large ratio of the scattering at 120° to that at 60°. The free cross-section model and the single-scattering calculation fail completely here. We note that this difference between the experimental and theoretical ratios (based on free cross sections) at these two angles is also seen in the data of Ref. 14.

The results for the effective number of nucleons presented in Table V have some features that can be qualitatively understood. Since the pion-nucleon total cross section is a maximum near 180 MeV (and the pion mean free path in nuclear matter a minimum), it would be expected that the effective number of nucleons would be smaller at 180 MeV than at 291 MeV, as is seen here. Since multiple scattering appears to be an important effect, it would also be expected that N_{eff}, as measured in this manner, would be fairly angle-independent, since much of the angular coherence is lost; this is also seen in the 290 MeV results.

A comparison of the single- and multiple-scattering curves shown in the figures indicates that there might be great difficulty in separating the single-scattered ("true quasielastic") pions from the multiply-scattered ones, in a single-arm experiment. The calculation indicates that the low-energy tails of the curves are due to the multiply-scattered pions, as would be expected, but the calculation is clearly not reliable enough to predict how much background due to multiple scattering would be found under the peak. At 60°, a large fraction of the peak, which lies in the kinematical region corresponding to single (quasielastic) scattering, actually corresponds to multiple scattering, according to the calculation. At 120°, the principal effect of multiple scattering appears to be a shifting of the peak to lower energy, as well as giving a low-energy tail, so that the separation into single and multiple scattering would be even more difficult.

IV. CONCLUSIONS

Many qualitative features of these data are fairly well reproduced by a model of incoherent multiple scattering of pions from a Fermi gas of nucleons contained inside a sphere of uniform density, as-

suming scattering probabilities based on free pion-nucleon angular distributions and total cross sections. These features include the general shapes of the scattered pion energy distributions, the π^+/π^- ratios, some characteristics of the ratios of the ^{44}Ca and ^{48}Ca cross sections to that of ^{40}Ca, and the ratios of the 120° to 60° cross sections at 291 MeV. A similar model involving single scattering, or a simple model based on free pion-nucleon cross sections, is considerably less successful in accounting for some of these features. Although the model makes many approximations, and in many ways is not very realistic, these results do suggest that multiple scattering is a very important feature of pion scattering in the quasielastic energy region. We feel that a more careful calculation which also incorporates multiple scattering would be very desirable in understanding these results.

This research was supported in part by the U. S. Department of Energy, the National Science Foundation, and the Robert A. Welch Foundation.

---

*Present address: University of South Carolina, Columbia, S. C. 29209.

[1]G. Jacob and Th. A. J. Maris, Rev. Mod. Phys. 45, 6 (1973); see also 38, 21 (1966).
[2]E. J. Moniz, Phys. Rev. 184, 1154 (1969).
[3]E. J. Moniz *et al.*, Phys. Rev. Lett. 26, 445 (1971).
[4]R. R. Silbar, Phys. Rev. C 11, 1610 (1975).
[5]B. J. Dropesky *et al.*, Phys. Rev. Lett. 34, 821 (1975); L. H. Batist *et al.*, Nucl. Phys. A254, 480 (1975); D. T. Chivers *et al.*, *ibid.* A126, 129 (1969); A. M. Poskanzer and L. P. Remsberg, Phys. Rev. 134, B779 (1964); P. L. Reeder and S. S. Markowitz, *ibid.* 133, B639 (1964).
[6]M. A. Moinester *et al.*, Phys. Rev. C 8, 2039 (1973); P. J. Karol *et al.*, Phys. Lett. 44B, 459 (1973); M. V. Yester *et al.*, *ibid.* 45B, 327 (1973); M. Zaider *et al.*, Phys. Rev. C 10, 938 (1974); B. J. Lieb *et al.*, Phys. Rev. Lett. 34, 965 (1975); N. P. Jacob, Jr. and S. S. Markowitz, Phys. Rev. C 13, 754 (1976).
[7]P. Varghese, thesis, University of Oregon, 1978 (Los Alamos Scientific Laboratory Report LA-7453-T).
[8]P. W. Hewson, Nucl. Phys. A133, 659 (1969); M. M. Sternheim and R. R. Silbar, Phys. Rev. Lett. 34, 824 (1975); J. Huffner *et al.*, Phys. Lett. 59B, 215 (1975).
[9]D. Robson, Ann. Phys. (N.Y.) 71, 277 (1972).
[10]F. Wilkinson, J. Phys. Soc. Jpn. Suppl. 24, 469 (1968).
[11]R. Seki, Nuovo Cimento 9A, 235 (1972).
[12]B. K. Jain and S. C. Phatak, Nucl. Phys. A302, 401 (1978).
[13]L. W. Swenson *et al.*, Phys. Rev. Lett. 40, 10 (1978).
[14]C. H. Q. Ingram in *Proceedings of the Second International Topical Conference on Meson-Nuclear Physics*, Houston, 1979 (AIP, New York, 1979), p. 455.
[15]H. A. Thiessen *et al.*, Los Alamos Scientific Laboratory Report, LA-4534-MS (unpublished).
[16]G. Rowe, M. Salomon, and R. H. Landau, Phys. Rev. C 18, 584 (1978).